

Suppression of Breast Cancer Metastasis Using Stapled Peptides Targeting the WASF Regulatory Complex

Cancer Growth and Metastasis
Volume 10: 1–9
© The Author(s) 2017
DOI: 10.1177/1179064417713197



John K Cowell¹, Yong Teng^{1,*}, N George Bendzunas², Roxan Ara¹,
Ali S Arbab¹ and Eileen J Kennedy²

¹Georgia Cancer Center, Augusta University, Augusta, GA, USA. ²Department of Pharmaceutical & Biomedical Sciences, College of Pharmacy, The University of Georgia, Athens, GA, USA.

ABSTRACT: The WASF3 gene facilitates the metastatic phenotype, and its inactivation leads to suppression of invasion and metastasis regardless of the genetic background of the cancer cell. This reliance on WASF3 to facilitate metastasis suggests that targeting its function could serve as an effective strategy to suppress metastasis. WASF3 stability and function are regulated by the WASF Regulatory Complex (WRC) of proteins, particularly CYFIP1 and NCKAP1. Knockdown of these proteins in vitro leads to disruption of the WRC and suppression of invasion. We have used mouse xenograft models of breast cancer metastasis to assess whether targeting the WRC complex suppresses metastasis in vivo. Stapled peptides targeting the WASF3-CYFIP1 interface (WAHM1) and the CYFIP1-NCKAP1 interface (WANT3) suppress the development of lung and liver metastases. Targeting these critical protein-protein interactions, therefore, could potentially be developed into a therapeutic strategy to control cancer cell invasion and metastasis.

KEYWORDS: Metastasis, stapled peptides, WASF3, suppression

RECEIVED: January 20, 2017. **ACCEPTED:** May 3, 2017.

PEER REVIEW: Seven peer reviewers contributed to the peer review report. Reviewers' reports totaled 1783 words, excluding any confidential comments to the academic editor.

TYPE: Original Research

FUNDING: The author(s) disclosed receipt of the following financial support for the research, authorship, and/or publication of this article: This work was supported in part by grants CA120510 (J.K.C.) and CA188439 (E.K.) from the National Institutes for Health and

pilot fund awards from Augusta University and University of Georgia. We are grateful to the staff of the Biomedicine core of the Georgia Cancer Center for assistance in Xenogen analysis in vivo.

DECLARATION OF CONFLICTING INTERESTS: The author(s) declared no potential conflicts of interest with respect to the research, authorship, and/or publication of this article.

CORRESPONDING AUTHOR: John K Cowell, Georgia Cancer Center, Augusta University, CN2116, 1410 Laney Walker Blvd, Augusta, GA 30912, USA. Email: jcowell@augusta.edu

Introduction

The majority of cancer deaths (>90%) result from consequences of metastatic spread,¹ and so targeting this aspect of disease progression could have a significant impact on survival. Many genes have been implicated in the development and promotion of the metastatic phenotype,² and we have previously demonstrated a central role for the WASF3 gene in this process.^{3,4} Knockdown of WASF3 in different cancer cell types leads to a suppression of invasion in vitro and metastasis in vivo.^{5,6} Thus, WASF3 offers a potential target in strategies to suppress metastasis.

WASF3 is part of a family of 3 proteins that are associated with actin cytoskeleton reorganization⁷ through a C-terminal domain that binds ARP2/3 and monomeric actin.⁸ Following WASF3 activation by a variety of kinases in response to extracellular stimuli,^{3,9,10} actin polymerization is promoted at the leading edge of the cell, which facilitates cell movement and invasion. WASF3 also promotes expression of genes involved in epithelial to mesenchymal transition, such as ZEB1¹¹ and members of the matrix metalloproteinase (MMP) family,⁴ through a signaling pathway that downregulates the KISS1 metastasis suppressor gene leading to activation of nuclear factor κB.¹² WASF3 is activated in response to hypoxia,¹³ as well as growth factor and cytokine stimulation of JAK2/STAT3 signaling.¹⁰ Under these conditions, WASF3 is recruited to the membrane and interacts with RAC, leading to relaxation of

inhibitory protein complexes and allowing recruitment of actin monomers to facilitate actin polymerization.¹⁴ WASF3 is held in an inactive, autoregulated form in unstimulated cells through engagement of a series of proteins including CYFIP1, NCKAP1, BRK1, and ABI1 through interactions with its N-terminus,^{15–17} forming the so-called WASF Regulatory Complex (WRC). The presence of this complex distinguishes the WASF proteins from other members of the superfamily, such as WASP and NWASP, which do not contain this motif and do not bind to RAC.¹⁸

CYFIP1 and NCKAP1 are important in maintaining the stability of the WRC as knockdown of either of these proteins leads to loss of all 3 proteins,¹⁴ presumably by destabilizing the entire WASF3 complex. There are currently no small-molecule inhibitors that target WASF3, and so we developed a series of stapled peptides that disrupt protein-protein interactions between members of the WRC, resulting in the suppression of invasion.^{14,19} Stapled peptides are constrained into an alpha-helical formation, which confers drug-like properties that are not intrinsic for unconstrained peptides, such as increased proteolytic stability, active uptake into cancer cells, and high specificity for the intended target due to the large interacting interface.^{20–23} In a previous in vitro study, we developed a stapled peptide that mimicked an alpha-helical interaction between WASF3 and CYFIP1.¹⁴ This peptide suppressed WASF3 phosphoactivation and led to the suppression of invasion in breast and prostate cancer cells. Knockdown of NCKAP1 also leads to the suppression of invasion¹⁹ but

* Present Address: Department of Oral Biology, Augusta University, Augusta, GA 30912, USA.



interacts with CYFIP1 rather than WASF3.^{24,25} Stapled peptides that target this interaction interface also lead to the suppression of invasion in vitro by destabilizing the WASF3 complex.¹⁹ To extend our in vitro studies, we now show that stapled peptides targeting protein-protein interactions that are essential for the maintenance of the WRC lead to the suppression of metastasis in an immunocompromised mouse model. These observations provide the proof-of-principle that targeting WASF3 function may serve as an effective strategy for suppressing metastasis in appropriate clinical settings.

Materials and Methods

Cell lines, in vivo tumor growth, and metastasis analysis

MDA-MB-231 breast cancer cell lines were directly obtained from American Type Culture Collection (Rockville, MD, USA). All cells were maintained in RPMI tissue culture medium supplemented with 5% fetal bovine serum (FBS; Fisher Scientific, Waltham, MA). Authentication of this cell line was verified using single nucleotide polymorphism-comparative genomic hybridization for characteristic cytogenetic changes.¹² The ATCC Cell Authentication Testing service also confirmed the identity of MDA-MB-231 (August 2015) using short tandem repeat DNA fingerprinting analysis. All experimental procedures were approved by the Institutional Animal Care and Use Committee (IACUC) of Augusta University. Six-week-old female NSG (NOD.Cg-Prkdc^{scid} Il2rg^{tm1Wjl}/SzJ) mice were purchased from the Jackson Laboratory (Bar Harbor, ME, USA) and maintained in accordance with IACUC guidelines. The animal experiments were performed using the NSG mouse model as described previously.²⁶ About 2×10^6 MDA-MB-231 cells were injected into the fourth mammary fat pads of groups of 4 NSG mice and tumors allowed to develop for 2 weeks before commencement of treatment with stapled peptides. The mice were euthanized after 5 weeks of treatment, and at the end of the experiment, dissected tumors were individually weighed. The lungs and livers were also removed from these mice and the number of nodules on the surface of the organs counted. For histological analyses, tissues were fixed in 10% neutral buffered formalin, embedded in paraffin blocks, sectioned at $5 \mu\text{m}$, and subjected to hematoxylin-eosin staining.

Invasion assays

Invasion assays were performed in Matrigel-coated modified Boyden chambers with $8 \mu\text{m}$ pore size filters (BD Biosciences, Rockville, MD, USA). In brief, the serum-starved cells were added in the upper chamber (5×10^4 cells per insert) and RPMI 1640 medium with 5% FBS was used as a chemoattractant in the lower chamber. After 24 hours of incubation, noninvading cells that remained on the upper surface of the filter were removed and the cells that had passed through the filter and

attached to the bottom of the membrane were stained with crystal violet cell stain solution (Millipore, Billerica, MA, USA). The number of cells per square millimeter were then counted and expressed as a percentage of cells in the control groups.

Stapled peptide synthesis

Peptides were synthesized on solid supports using Fmoc chemistry, and ring-closing metathesis was performed as previously described.¹⁴ Peptides were subsequently purified by reversed-phase high-performance liquid chromatography. The masses of the purified peptides are as follows (asterisks represent (S)-2-(4-pentenyl) alanine): WAHM1 (FAM-PEG₃-LEK*TNS*LAKIIRQL) = 2423.4 (expected mass = 2423.8), WANT3-v1 (FAM- β A-VLLRNA*HAV*K) = 1798.2 (expected mass = 1799.0), WANT3-v2 (FAM- β -VLLRN*YHA*YK) = 1954.5 (expected mass = 1955.2), WANT3-v3 (FAM- β A-V*LRN*YHAVYK) = 1940.7 (expected mass = 1941.2), and WANT3-v1 scramble (FAM- β A-AKALVH*LRN*V) = 1798.8 (expected mass = 1799.0). (FAM- β A-AKALVH*LRN*V) = 1798.8 (expected mass = 1799.0). Peptides synthesized in preparation for radiolabeled iodination are as follows: WANT3-v1 Tyr-N-term (Y-PEG₃-VLLRNA*HAV*K) = 1721.6 (expected mass = 1722.1) and WAHM1 Tyr-N-term (Y-PEG₃-LEK*TNS*LAKIIRQL) = 2228.1 (expected mass = 2228.7).

Bioluminescence imaging

In mouse xenografts, we used luciferase-expressing breast cancer cells for in vivo bioluminescence imaging using the Xenogen IVIS imaging systems. Breast cancer cells expressing the luciferase gene were implanted into the fat pads of 5-week-old NOD/SCID mice. These mice were imaged at intervals of between 8 and 35 days (see text) during the treatment schedule to monitor tumor behavior. Prior to imaging, the animals were anesthetized with a mixture of oxygen (1:1) and 2.5% isoflurane in a clear induction chamber. After initial exposure to anesthesia, the mice were positioned in the supine position inside the imaging system: throughout the session, animal anesthetization was maintained at ~1.25% isoflurane.

Blood clearance, whole-body biodistribution, and in vivo imaging

Peptides were labeled with iodine 125 (¹²⁵I) radioisotope (PerkinElmer, Waltham, MA, USA; product no. NEZ033H005MC) using typical Pierce iodination beads (Thermo Scientific, Waltham, MA, USA; cat. no. 28665) according to the manufacturer's protocol. In brief, the total amount of beads needed for the reaction was determined based on the amount of peptide to be labeled (1 bead was added to the reaction for every $50 \mu\text{g}$ of peptide). After washing with

phosphate-buffered saline (PBS) and drying, the I^{125} solution was incubated with the beads for 5 minutes. The measured peptide solution in PBS was then added and allowed to react for 15 to 20 minutes. The beads were then separated from the reaction vials using long forceps, and the I^{125} -labeled peptides were dialyzed through ultracentrifuge filters (1K cutoff) to separate free from bound I^{125} . Labeling efficiency was determined by thin-layer chromatography with proper eluent (85% methanol).

Radiolabeled peptides were injected into the mouse tail vein and blood was collected from the opposite tail vein 5 minutes, 30 minutes, 60 minutes, 3 hours, and 24 hours after intravenous administration of labeled peptide. The blood was weighed and radioactivity was measured using a gamma counter. Radioactivity was normalized to the weight of the collected blood (activity/g) and plotted to determine the blood half-life.

Biodistribution using single-photon emission computed tomography. The I^{125} -labeled peptides were injected (50 μ g) intravenously. The distribution of radioactivity in normal and tumor tissues was analyzed using whole-body single-photon emission computed tomography (SPECT) with a dedicated 4-headed NanoScan, high-sensitivity microSPECT/CT 4R (Mediso, Boston, MA, USA) fitted with high-resolution multi-pinhole (total 100) collimators. The microSPECT has a wide range of energy capabilities from 20 to 600 keV, with a spatial resolution of 275 μ m. The images were obtained using 60 projection images with 60 seconds/projection, with medium field of view. Attenuation was corrected using concurrent computed tomographic (CT) images which were reconstructed with low iteration and low filtered back-projection.

Whole-body distribution of radioactivity was measured using ImageJ software (National Institutes of Health) by merging all reconstructed images and by making irregular regions of interest (ROI) encompassing the whole body of the animals. Radioactivity in the tumor (merging all sections containing tumor guided by CT images) was also measured by making irregular ROIs.

Following the 72-hour SPECT imaging, animals were euthanized and different tissues including tumors were collected and weighed, and then radioactivity was measured using a gamma counter and normalized to the weight of the tissues.

Results

Suppression of metastasis in mouse breast cancer xenograft models

The WRC is critical for the stability of the WASF3 protein. Targeting the interface between the CYFIP1 and WASF3 proteins using stapled peptides (WAHM1/2) led to the suppression of activation of WASF3 and loss of invasion *in vitro*.¹⁴ To extend these studies to mammalian models, we evaluated the ability of the WAHM1 peptide to suppress metastasis in mouse xenograft models. We^{14,26} and others²⁷ have previously shown that breast cancer cells, when injected into the mammary fat

pads of NSG mice, will develop as primary tumors and rapidly metastasize to the lungs within 1 to 2 months, obviating the need to remove the primary tumor during the experimental process. We have also shown that genetic knockdown of WASF3 in MDA-MB-231 cells leads to a significantly reduced metastasis potential in mouse xenograft models.⁵ To evaluate the ability to modulate metastasis in this NSG model using stapled peptides targeting the WRC, we implanted MDA-MB-231 cells, which had been stably transfected with the luciferase gene, into the fourth mammary fat pad of NSG mice. Tumors were allowed to develop for 2 to 3 weeks and the mice were then treated with WAHM1. We have previously demonstrated that these stapled peptides are relatively stable in serum for up to 3 days,¹⁴ and so the mice were treated every other day at 2 concentrations, 15 and 30 mg/kg, delivered intraperitoneally. After treatment for only 2 weeks with the higher concentration, however, the mice showed significant morbidity and weight loss, and so treatment at this dose was discontinued. Tumor growth in the treated and control mice was measured using calipers and showed parallel development over the first 4 weeks. After 5 weeks, however, the stapled peptide-treated mice showed delayed tumor development compared with the control-treated mice (Figure 1A). After 5 weeks, 2 mice being treated with 15 mg/kg WAHM1 were injected with luciferin and, after 12 to 15 minutes, imaged using the Xenogen bioluminescence instrument. As shown in Figure 1A, cancer cells grew locally and spread throughout the body rapidly in mice treated with the vehicle alone (dimethyl sulfoxide [DMSO]). In contrast, in the cohort treated with WAHM1 peptides, there was a significant reduction in the observed extent of dissemination of tumor cells (Figure 1B), suggesting reduced metastasis. At the conclusion of the *in vivo* treatments, mice were killed and the weight of the tumors in the WAHM1-treated mice showed a significant reduction compared with control tumors (Figure 1C). The overall body weight was also reduced. Analysis of the lungs from these mice (Figure 1D) showed a significant reduction in the number of surface tumor nodules in the WAHM1-treated mice, compared with the vehicle control.

Targeting the CYFIP1-WASF3 interaction with stapled peptides clearly shows suppression of metastasis. During the course of our studies, we also demonstrated that inactivation of NCKAP1 using short hairpin RNA (shRNA) led to destabilization of the WASF3 protein complex and reduced invasion potential.¹⁹ NCKAP1, however, does not interact directly with WASF3.²⁴ Analysis of the crystal structure of the WRC shows that NCKAP1, instead, interacts directly with the CYFIP1 protein, which is the target for RAC1. Using stapled peptides targeting the CYFIP1-interacting interface on NCKAP1, we identified an inhibitor peptide (WANT3) that led to the suppression of invasion as a result of destabilization of the total WASF3 complex.¹⁹ In attempts to improve the efficacy of WANT3, we designed 3 variants

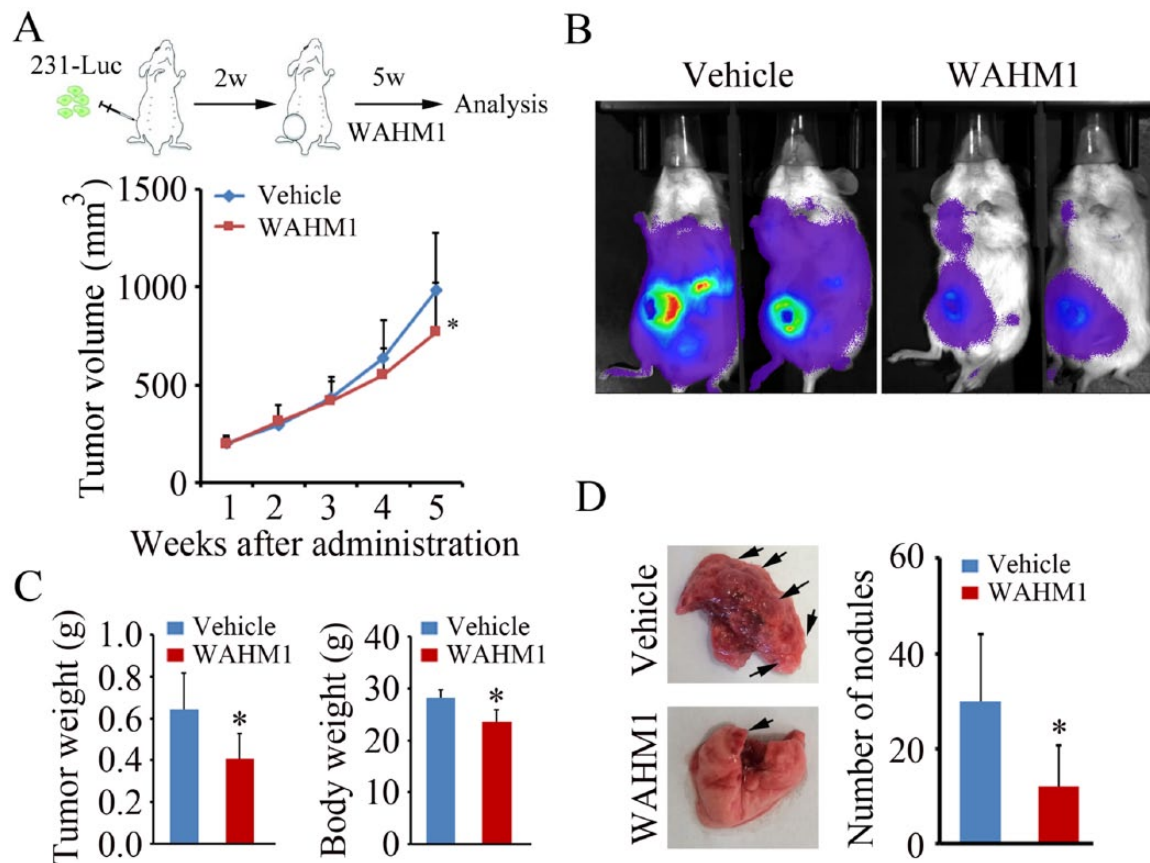


Figure 1. Targeting the CYFIP1-WASF3 interface suppresses metastasis in vivo. (A, above) Scheme of treatment with the WAHM1 peptide. Injections of stapled peptides began 2 weeks after the injection of tumor cells and continued for a further 5 weeks. (A, below) Primary tumor volume was measured at weekly intervals where there was a significant reduction in tumor size after 5 weeks ($*P < .05$). (B) Bioluminescence imaging after 5 weeks suggests more extensive spread of the tumor in animals treated with vehicle alone compared with animals treated with the WAHM1 peptide. (C) On completion of the experiments, tumor weight was significantly smaller in the WAHM1-treated animals as was the overall body weight. (D) On completion of the treatment regimen, analysis of the lungs shows a significant reduction in the number of surface tumor nodules in the WAHM1-treated animals.

(V1-3) by altering the position of the staple within the parent peptide (see the “Materials and Methods” section). Scrambled peptides were also prepared as controls. These peptides were first analyzed for their relative ability to suppress invasion in vitro using transwell assays. As shown in Figure 2A, variants V2 and V3 proved significantly less efficient than the parent WANT3 peptide, although they produced a significant reduction in invasion compared with the scrambled controls. In contrast, variant V1 was significantly more effective in suppressing invasion compared with WANT3. As a result, the WANT3-v1 variant was used in in vivo studies following the protocol described above for WAHM1, where MDA-MB-231 cells were injected into NSG mice and then treated with the stapled peptides at 15 mg/kg every other day. Animals were imaged after 8, 15, and 28 days (Figure 2B), where again the mice treated with the scrambled control showed extensive dissemination from the primary site. In contrast, the WANT3-v1-treated mice showed smaller primary tumors and reduced dissemination. On termination of treatment, the mice were killed and the lungs removed. It was found that the number of tumor nodules was significantly reduced in the WANT3-v1-treated

mice. Analysis of the livers in these mice showed an even more significant reduction in the number of nodules (Figure 2C). These observations were further confirmed using histopathological analysis of the lungs and livers (Figure 2D).

During these experiments, tumor growth was monitored weekly using calipers to measure tumor volume. As shown in Figure 1A, the tumors initially grew at a comparable rate in WAHM1-treated mice; however, the relative size of the tumors diverged after 4 weeks and the overall weight of the primary tumors was significantly reduced after 5 weeks. However, the tumor sizes were indistinguishable for the first 4 weeks regardless of treatment. WAHM1 treatment of breast cancer cells in vitro does not affect cell proliferation, and Ki67 staining of the WAHM1-treated tumors showed no significant difference (25% vs 22%) in the proliferation potential compared with control mice (Figure 3). We previously suggested that reduced tumor size in MDA-MB-231 WASF3 knockdown cells⁵ leads to reduced vascularization in xenografts. As shown in Figure 3, using the endothelial cell-specific anti-CD31 antibody, there was a significant reduction after 5 weeks in the number and size of microvessels throughout the primary tumors in the WAHM1-treated mice. Thus, targeting the WRC in vivo demonstrates

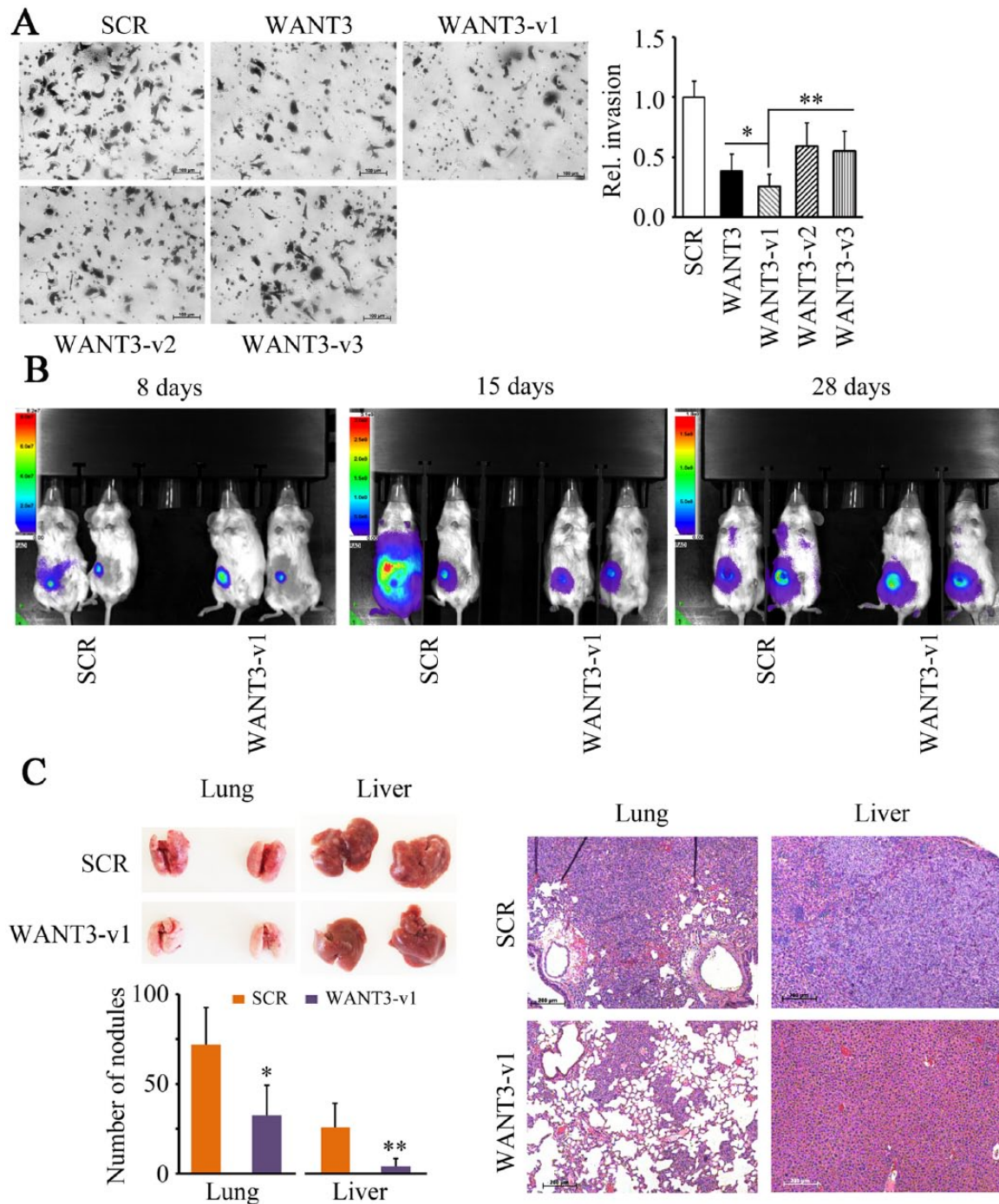


Figure 2. Targeting the NCKAP1-CYFIP1 interface suppresses metastasis in vivo. (A) Comparison of invasion potential of MDA-MB-231 cells using transwell assays comparing the original WANT3 peptide with 3 variants (v1-3) shows that the WANT3-v1 peptide is more efficient than the parent WANT3 peptide. * $P < .05$, ** $P < .01$. (B) Relative intensities in the bioluminescence analysis of mice treated with the WANT3-v1 peptide show reduced spread of tumor cells over 28 days compared with mice treated with the scrambled (SCR) peptide. After completion of the treatment regimen, analysis of the lungs and liver shows reduced numbers of surface nodules (C, left) which was confirmed by histopathological analysis showing extensive infiltration in lung and liver in mice treated with the SCR control compared with the WANT3-v1 peptide (C, right). * $P < .05$, ** $P < .01$.

not only reduced metastasis but also suppression of neovascularization in the primary tumor.

Biodistribution and blood clearance

We have recently demonstrated that the WAHM stapled peptides are relatively stable over at least 3 days in vitro in the

presence of serum.¹⁴ As these stapled peptides may have the potential to serve as antimetastasis agents, it is important to establish their biodistribution and clearance in vivo. To do this, we used SPECT analysis following I^{125} labeling of the WAHM1 and WANT3-v1 stapled peptides. For I^{125} labeling, modified versions of WAHM1 and WANT3-v1 were generated where a tyrosine residue was added to the N-terminus

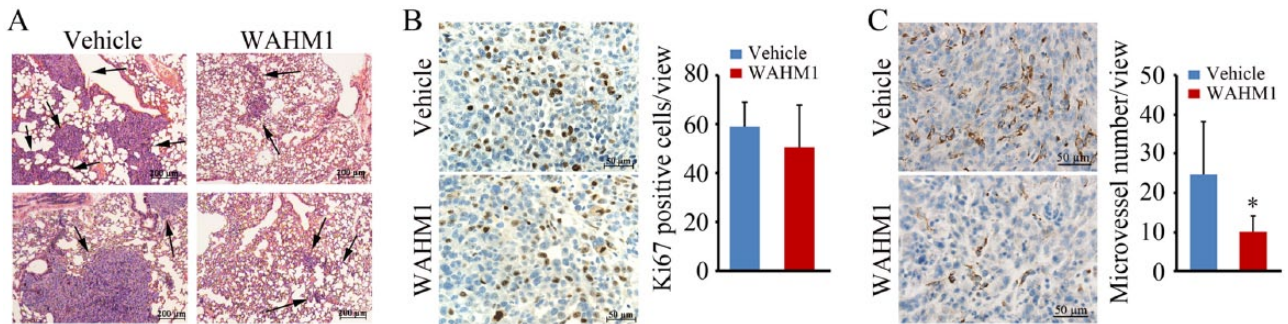


Figure 3. (A) Histopathological analysis (hematoxylin-eosin stained) of tumors derived from MDA-MB-231 cells in NSG mice shows large tumors distributed through the lungs in animals treated with vehicle alone but only small and infrequent tumors in the lungs of animals treated with the WAHM1 stapled peptide. (B) Analysis of Ki67 staining in primary tumors in the fat pads shows no significant difference in mice treated with either the vehicle or the WAHM1 peptide. (C) Analysis of tumor vasculature using CD31 antibodies shows a significant reduction in the number of microvessels in the primary tumors treated with the WAHM1 peptide compared with animals treated with the vehicle alone. * $P < .05$. Images in B and C were counterstained with hematoxylin.

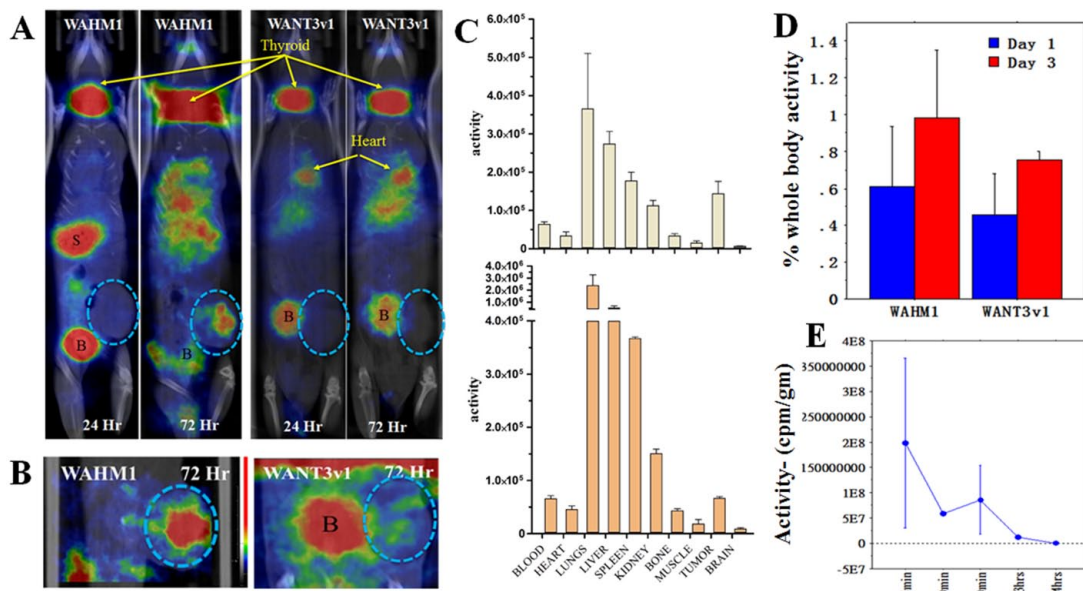


Figure 4. Biodistribution of stapled peptides in tumor xenografts and organs. (A) Z-stack reconstruction of single-photon emission computed tomographic imaging of mice treated with WAHM1 shows dominant uptake in the thyroid (T), stomach (S), and bladder (B). After 72 hours, radioactivity levels in the stomach and bladder have dissipated, revealing significant uptake in the lungs and liver as well as in the tumor (shown exclusively [circled in B] in the respective insets). Treatment with the WANT3-v1 peptide shows dominant uptake in the thyroid and the bladder and in this case in the heart. After 72 hours, there are higher levels in the lungs and liver and clearance is still in process through the bladder (A). (C) Quantitation of I¹²⁵ tracer levels, measured as radioactivity per gram of tissue in the major organs following treatment with WAHM1 (above) and WANT3-v1 (below), shows significant uptake in tumors after 72 hours. (D) When tumor uptake is expressed as a percentage of body weight, a progressive increase in tracer levels is seen between 24 and 72 hours for both peptides. (E) Radioactivity levels were measured in the blood of 3 animals after a single injection of I¹²⁵-labeled peptides over a 24-hour period showing a half-life of 20 to 30 minutes.

followed by a short PEG₃ linker. The N-terminal tyrosine was then radiolabeled with I¹²⁵ using Pierce iodination beads. This chemical tracer was then used to monitor the distribution of the peptide throughout the mouse body using SPECT analysis (Figure 4). To extend the biodistribution observations from normal tissues to tumors, MDA-MB-231 xenografts were established in the mammary fat pads 2 weeks prior to

treatment. Using 4 to 5 mice in each group, I¹²⁵-labeled peptides were injected and the distribution of radioactivity was then assessed over 72 hours as described in the “Materials and Methods” section. The SPECT imaging was performed at 24 and 72 hours. As seen in Figure 4, after 24-hour treatment with WAHM1, reduced and free iodine localizes to the thyroid and stomach as expected, due to active iodine transporters in these

organs, as well as the bladder, which is a major clearance route. Because of the intensity normalization over the image, apparent uptake in the tumors, lungs, and liver was suppressed because of the lower levels (activity) in these sites. After 72 hours, however, the majority of the unbound iodine had cleared from the stomach and bladder and significant uptake was seen in the tumor (Figure 4) as well as in the lungs and liver. The WANT3-v1 peptide behaved slightly differently in this *in vivo* analysis where, after 24 hours, high levels were again seen not only in the thyroid and bladder but also in the heart. Retention in the heart was maintained up to 72 hours suggesting retention in the blood system. Significant levels were also seen in the liver after 72 hours, and there was still radioactive tracer in the bladder in these mice, suggesting free or cleaved peptide is still present. Tumor uptake of the WANT3-v1 peptide as assessed by SPECT was again masked by the relatively high levels of tracer in the other organs but focused imaging in the flank of the animal where the tumor was created showed uptake at reasonable levels (Figure 4). From these studies, we noted that tumor uptake of the WAHM1 peptide was significantly greater than for the WANT3-v1 peptide, which may be due to dominant retention in the lungs of the latter peptide as the unlinked WANT3-v1 peptide was more efficient in suppressing invasion *in vitro* and *in vivo* than WAHM1.¹⁹ However, it is possible that the WANT3-v1 peptide may undergo proteolytic degradation and lose its N-terminal radiolabel.

After 72 hours, mice were killed and various organs (blood, brain, lungs, liver, spleen, kidneys, bone, muscle, and tumor) were isolated, and the radioactivity per gram of tissue was quantified using gamma counting. As shown in Figure 4, the distribution of the peptides mimicked the distribution seen by SPECT with highest activities seen in the liver and lungs, as expected, although there was significant tracer in the tumors. This was consistent with the imaging data where WAHM1 uptake was greater than that of WANT3-v1. When the relative levels of radioactivity per gram of tissue were determined in major organs and the tumors, it was clear, however, that significant levels of the tracer were seen in the tumors (Figure 4C and D). In fact, the tumors showed one of the most significant uptakes of the tracer. In parallel, we analyzed peptide clearance of WANT1 from the blood by assessing radioactivity levels in blood samples over a time course ranging from 5 minutes to 24 hours post injection with the radiolabeled peptide using another cohort of mice. This provided an estimate of the clearance rate of the peptides after single injections (Figure 4E), indicating the blood half-life of the peptide was approximately 20 to 25 minutes.

Discussion

As metastasis is the overwhelming cause of cancer deaths, designing ways to suppress or delay this progression event

could have a significant impact on overall survival in patients with cancer. We have previously demonstrated the unique role of WASF3 in this process,¹⁴ supported by mechanistic studies,^{3-5,9-12} identifying it as a rational target to suppress metastasis. We now show that our stapled peptide strategy, targeting the WRC, provides one potential approach to suppress metastasis *in vivo*. We have defined 2 targets that appear to have the same ability to affect lung and liver metastasis, even though *in vitro* studies suggest that their mechanism of action is slightly different. WAHM1 suppresses phosphoactivation of WASF3,¹⁴ which is required for its function,⁹ whereas WANT3 leads to destabilization of the WRC protein complex.¹⁹ Regardless of the specific mechanism of action, both stapled peptides show equally efficient suppression of invasion *in vitro* and metastasis *in vivo*, suggesting a therapeutic opportunity for this approach. Stapled peptides have distinct advantages over traditional peptides in that they are nonimmunogenic, readily penetrate cells through active transport, and are more stable in serum.²⁸ In addition, they can target intracellular surfaces that are not accessible to small molecules by providing a larger interaction surface for binding. We have already shown that a second-generation peptide with a modified staple position (WANT3-v1) suppresses invasion more efficiently. If this compound can be further refined through modifications to increase stability, subsequently optimized versions may allow for less frequent administration with potentially fewer side effects. Notably, the 15 mg/kg dose used for the current peptides tested did not result in any significant observable side effects on the mice. In the animal studies, we injected the stapled peptides intraperitoneally, as in our hands multiple intravenous injections led to localized thickening of the tail vein due to the DMSO solute and made repeated, successive injections difficult. The other shortcoming of the regimen described here is the short retention time seen in the blood system for the WAHM1 peptide, which we calculated to be ~30 minutes, even though under these circumstances uptake of the peptides was significant in the tumors. Future optimization of these peptides could lead to increased retention time and possibly increased delivery to the tumor.

An obvious concern about targeting WASF3 to suppress metastasis is the potential side effects that might result from targeting the WRC, which is also present in 2 other WASF family members that have related functions.²⁸ WASF3 is a member of superfamily of genes that includes the WASP proteins¹⁸ that also regulate actin polymerization, but the WASF subfamily uniquely contains the WRC domain, which is the target of WAHM1 and WANT3. The other 2 WASF family members, however, have different expression profiles⁷ and are regulated by different transcription factors¹⁰ even though they retain the WRC domain. Importantly, our previous studies demonstrated that shRNA knockdown of the other members of the WASF3 family, in a variety of

cancer cell types, did not have an obvious visible phenotype even though this affected their stability.¹⁴ Furthermore, knockdown of WASF1 and WASF2 in breast cancer cells did not lead to suppression of invasion,¹⁴ further supporting a novel and unique function for WASF3 in the regulation of this phenotype.

Our preliminary studies using both the WAHM1 and WANT3-v1 peptides demonstrate significant tumor uptake over 72 hours after only a single treatment, providing supportive evidence for the ability of these peptides to suppress metastasis. Extending the retention time up to 3 hours could result in far better distribution into tumors. The biodistribution throughout the animal also provides encouraging evidence for limited side effects on the host. During the treatment of animals at the lower dose, there were no obvious observable adverse effects, and the biodistribution showed relatively little uptake beyond the immediate destinations following intravenous injection (lungs and liver). Uptake by the thyroid is likely due to the preferential uptake of free and cleaved I¹²⁵ used during the radiolabeling process, and clearance of this tracer occurs quickly through the bladder.

The experiments described in this study show that even after tumors have developed, there is a significant reduction in metastasis, although it was clear that suppression was not complete under these circumstances. Although this system cannot be used to evaluate whether targeting the WRC affects dissemination, colonization, or growth at the distant site, it demonstrates that, even after development of the tumor, metastasis is suppressed and the metastatic burden is reduced in the mouse. This may be due to its demonstrated ability to suppress proteins such as MMPs,³ which are required for invasion and metastasis, and indirectly, we have shown that these mechanisms are affected. In a zebrafish model, for example, intravasation by tumor cells is seen when human cells are injected into the perivitelline space associated with the yolk sac. Knockdown of WASF3 in the same cells shows a highly significant reduction in the number of cells that disseminate through the fish, suggesting compromised ability to access the vasculature.²⁹ At the other end of the metastasis process, we have also shown that when WASF3 knockdown cells are injected directly into the vasculature, and therefore bypass the intravasation process, their ability to form tumors in the lungs is significantly reduced, suggesting a defect in extravasation.⁵ In a clinical setting, therefore, treating the patient with agents to suppress metastasis, even after the diagnosis of metastatic cancer, may have a beneficial effect by reducing the metastatic burden. Alternatively, in cases where diagnosis of early-stage cancer, eg, stage IIA breast cancer, before metastasis is suspected, antimetastatic agents could provide an adjuvant means of suppressing metastasis of rare tumor cells with this phenotype. This type of adjuvant therapy could also address the issue of tumor cell dormancy³⁰ where metastatic cells are already disseminated but lie dormant before colonizing a distant organ. As we know that inactivation of WASF3 suppresses both

extravasation and local invasion, a WASF3 suppressor may prevent colonization of the distant organ years after the removal of the primary tumor.

In this report, we provide the proof-of-principle evidence that stapled peptides targeting the WRC can effectively suppress metastasis in vivo, suggesting the basis of an antimetastasis therapy. During the course of these experiments, we encountered circumstances that can now potentially be overcome through specific modification of the structure and/or sequence of the peptides to render them less susceptible to proteolytic cleavage while enhancing half-life circulation and biodistribution. Building on these observations, future optimization of these peptides may potentially have greater efficacy in suppressing metastasis, especially in patients with early-stage tumors that have a high risk of recurrence as locally invasive or distantly metastasized tumors. Although these pilot studies were conducted in murine xenografts of human breast cancer cells, we have also shown that suppression of WASF3 leads to a reduction in metastasis in prostate cancer⁶ and invasion of colon cancer cells,¹⁹ as well as several other cancer cell types (unpublished results). It is possible, therefore, that targeting WASF3 may have a broad effect in suppressing metastasis in many tumor types that share the commonality of high-level expression of WASF3.

Acknowledgements

We are grateful to Laura Hanold for technical assistance with peptide generation and to Mohammad H Rashid and Asm Iskander for assistance in the preparation of the I¹²⁵ radioactive labeling study.

Author Contributions

Study design and concept were created by JKC and EK. In vivo mouse experiments were performed by YT, and biodistribution studies were performed by RA and ASA. Stapled peptides were designed and created by NGB and EK. JKC and EK wrote the manuscript.

REFERENCES

1. Siegel R, Naishadham D, Jemal A. Cancer statistics, 2012. *Cancer J Clin.* 2012;62:10–29.
2. Nguyen DX, Massagué J. Genetic determinants of cancer metastasis. *Nat Rev Genet.* 2007;8:341–352.
3. Sossey-Alaoui K, Ranalli TA, Li X, Cowell JK. WAVE3 promotes cell motility and invasion through the regulation of MMP-1, MMP-3, and MMP-9 expression. *Exp Cell Res.* 2005;308:135–145.
4. Sossey-Alaoui K, Li X, Ranalli TA, Cowell JK. WAVE3-mediated cell migration and lamellipodia formation are regulated downstream of phosphatidylinositol 3-kinase. *J Biol Chem.* 2005;280:21748–21755.
5. Sossey-Alaoui K, Safina A, Li X, et al. Down-regulation of WAVE3, a metastasis promoter gene, inhibits invasion and metastasis of breast cancer cells. *Am J Pathol.* 2007;170:2112–2121.
6. Teng Y, Ren M, Cheney R, Sharma S, Cowell JK. Inactivation of the WASF3 gene in prostate cancer cells leads to suppression of tumorigenicity and metastasis. *Br J Cancer.* 2010;103:1066–1075.
7. Sossey-Alaoui K, Nowak N, Cowell JK. Genomic organization and expression profile of the human and mouse WAVE gene family. *Mamm Genome.* 2003;14:314–322.

8. Takenawa T, Miki H. WASP and WAVE family proteins: key molecules for rapid rearrangement of cortical actin filaments and cell movement. *J Cell Sci.* 2001;114:1801–1809.
9. Sossey-Alaoui K, Li X, Cowell JK. c-Abl-mediated phosphorylation of WAVE3 is required for lamellipodia formation and cell migration. *J Biol Chem.* 2007;282:26257–26265.
10. Teng Y, Ghoshal P, Ngoka L, Mei Y, Cowell JK. Critical role of the WASF3 gene in JAK2/STAT3 regulation of cancer cell invasion. *Carcinogenesis.* 2013;34:1994–1999.
11. Teng Y, Mei Y, Hawthorn L, Cowell JK. WASF3 regulates miR-200 inactivation by ZEB1 through suppression of KISS1 leading to increased invasiveness in breast cancer cells. *Oncogene.* 2014;33:203–211.
12. Teng Y, Liu M, Cowell JK. Functional interrelationship between the WASF3 and KISS1 metastasis-associated genes in breast cancer cells. *Int J Cancer.* 2011;129:2825–2835.
13. Ghoshal P, Teng Y, Lesoon L, Cowell JK. HIF1A induces expression of the WASF3 metastasis associated gene under hypoxic conditions. *Int J Cancer.* 2012;131:E905–E915.
14. Teng Y, Bahassan A, Dong D, et al. Targeting the WASF3-CYFIP1 complex using stapled peptides suppresses cancer cell invasion. *Cancer Res.* 2016;76:965–973.
15. Steffen A, Rottner K, Ehinger J, et al. Sra-1 and Nap1 link Rac to actin assembly driving lamellipodia formation. *EMBO J.* 2004;23:749–759.
16. Stovold CF, Millard TH, Machesky LM. Inclusion of Scar/WAVE3 in a similar complex to Scar/WAVE1 and 2. *BMC Cell Biol.* 2005;6:11.
17. Gautreau A, Ho HY, Li J, Steen H, Gygi SP, Kirschner MW. Purification and architecture of the ubiquitous Wave complex. *Proc Natl Acad Sci USA.* 2004;101:4379–4383.
18. Takenawa T, Suetsugu S. The WASP-WAVE protein network: connecting the membrane to the cytoskeleton. *Nat Rev Mol Cell Biol.* 2007;8:37–48.
19. Teng Y, Qin H, Bahassan A, Bendzun NG, Kennedy EJ, Cowell JK. The WASF3-NCKAP1-CYFIP1 complex is essential for breast cancer metastasis. *Cancer Res.* 2016;76:5133–5142.
20. Verdine GL, Walensky LD. The challenge of drugging undruggable targets in cancer: lessons learned from targeting BCL-2 family members. *Clin Cancer Res.* 2007;13:7264–7270.
21. Guerlavas V, Sawyer TK. Advancements in stapled peptide drug discovery and development. *Ann Rev Med Chem.* 2014;49:331–345.
22. Schafmeister CE, Po J, Verdine GL. An all-hydrocarbon cross-linking system for enhancing the helical and metabolic stability of peptides. *J Am Chem Soc.* 2000;122:5891–5892.
23. Kutchukian PS, Yang JS, Verdine GL, Shakhnovich EI. All-atom model for stabilization of alpha-helical structure in peptides by hydrocarbon staples. *J Am Chem Soc.* 2009;131:4622–4627.
24. Chen B, Brinkmann K, Chen Z, et al. The WAVE regulatory complex links diverse receptors to the actin cytoskeleton. *Cell.* 2014;156:195–207.
25. Chen Z, Borek D, Padrick SB, et al. Structure and control of the actin regulatory WAVE complex. *Nature.* 2010;468:533–538.
26. Teng Y, Ren X, Li H, Shull A, Kim J, Cowell JK. Mitochondrial ATAD3A combines with GRP78 to regulate the WASF3 metastasis-promoting protein. *Oncogene.* 2016;35:333–343.
27. Iorns E, Drews-Elger K, Ward TM, et al. A new mouse model for the study of human breast cancer metastasis. *PLoS ONE.* 2012;7:e47995.
28. Suetsugu S, Yamazaki D, Kurisu S, Takenawa T. Differential roles of WAVE1 and WAVE2 in dorsal and peripheral ruffle formation for fibroblast cell migration. *Dev Cell.* 2003;5:595–609.
29. Teng Y, Xie X, Walker S, White DT, Mumm JS, Cowell JK. Evaluating human cancer cell metastasis in zebrafish. *BMC Cancer.* 2013;13:453.
30. Giaccotti FG. Mechanisms governing metastatic dormancy and reactivation. *Cell.* 2013;155:750–764.